JACS
JOURNAL OF THE AMERICAN CHEMICAL SOCIETY

Article

pubs.acs.org/JACS

Multiple Complexes of Long Aliphatic *N*-Acyltransferases Lead to Synthesis of 2,6-Diacylated/2-Acyl-Substituted Glycopeptide Antibiotics, Effectively Killing Vancomycin-Resistant Enterococcus

Syue-Yi Lyu,[†,‡] Yu-Chen Liu,[†] Chin-Yuan Chang,[†] Chuen-Jiuan Huang,[∥] Ya-Huang Chiu,[§] Chun-Man Huang,[†,‡] Ning-Shian Hsu,[†] Kuan-Hung Lin,[†] Chang-Jer Wu,[§] Ming-Daw Tsai,[∥] and Tsung-Lin Li*[,†,⊥]

[†]Genomics Research Center, Academia Sinica, Taipei 115, Taiwan

[‡]Department of Microbiology and Immunology, National Yang-Ming University, Taipei 112, Taiwan

[§]Department of Food Science, National Taiwan Ocean University, Keelung 202, Taiwan

[∥]Institute of Biological Chemistry, Academia Sinica, Taipei 115, Taiwan

[⊥]Biotechnology Center, National Chung Hsing University, Taichung 402, Taiwan

Supporting Information

ABSTRACT: Teicoplanin A2-2 (Tei)/A40926 is the last-line antibiotic to treat multidrug-resistant Gram-positive bacterial infections, e.g., methicillin-resistant *Staphylococcus aureus* (MRSA) and vancomycin-resistant enterococcus (VRE). This class of antibiotics is powered by the *N*-acyltransferase (NAT) Orf11*/Dbv8 through *N*-acylation on glucosamine at the central residue of Tei/A40926 pseudoaglycone. The NAT enzyme possesses enormous value in untapped applications; its advanced development is hampered largely due to a lack of structural information. In this report, we present eight high-resolution X-ray crystallographic unary, binary, and ternary complexes in order to decipher the molecular basis for NAT's functionality. The enzyme undergoes a multistage conformational change upon binding of acyl-CoA, thus allowing the uploading of Tei pseudoaglycone to enable the acyl-transfer reaction to take place in the occlusion between the N- and C-halves of the protein. The acyl moiety of acyl-CoA can be bulky or lengthy, allowing a large extent of diversity in new derivatives that can be formed upon its transfer. Vancomycin/synthetic acyl-*N*-acetyl cysteamine was not expected to be able to serve as a surrogate for an acyl acceptor/donor, respectively. Most strikingly, NAT can catalyze formation of 2-*N*,6-*O*-diacylated or C6→C2 acyl-substituted Tei analogues through an unusual 1,4-migration mechanism under stoichiometric/solvational reaction control, wherein selected representatives showed excellent biological activities, effectively counteracting major types (VanABC) of VRE.

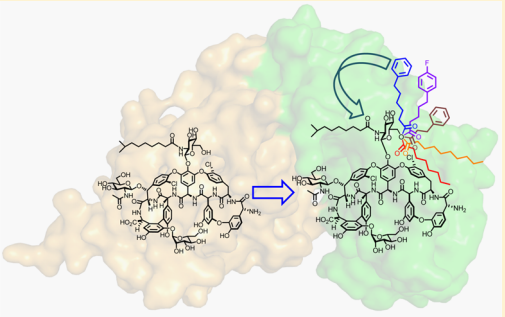

I

INTRODUCTION

Lipoglycopeptide antibiotics teicoplanin A2-2 (**1**, referred to here as teicoplanin, Tei) and A40926 (**2**) feature a long aliphatic acyl side chain attached to glucosamine at the central 4-hydroxylphenylglycine (4Hpg) of the Tei/A40926 pseudoaglycone scaffold (**3**) (Figure 1).[1] The gene products *orf11** and *dbv8* were characterized to be *N*-acyltransferases (NATs) responsible for *N*-acylation in the biosynthesis of Tei and A40926, respectively. This modification galvanizes the effectiveness of lipoglycopeptide antibiotics in exterminating methicillin/multidrug-resistant *Staphylococcus aureus* (MRSA).[2] The potential for new applications of the NAT enzyme has since been implied, but without elaboration and detail.[3−5] Mining the protein sequences from public databases returned no hits, suggesting that the enzyme adapts a new structural architecture distinct from typical NAT. It is thus of great interest to know how the two bulky substrates, decanoyl-CoA (**4**) and Tei/A40926 pseudoaglycone (**3**), are recruited and how the acyl-transfer reaction is executed. Solving enzyme complex structures at various reaction stages seemed the best way to answer these questions. In parallel with the structural determination, we discovered two unusual acyl-transfer reactions, granting a new chemoenzymatic strategy. This approach allows access to new classes of products that would be extremely difficult to obtain by other means and that offer improved and complementary profiles for antimicrobial drug discovery efforts.

MATERIALS AND METHODS

Protein expression, purification, and confirmation of purity were performed according to standard protocols.[6−8] Acyl-CoA analogues were chemically synthesized as described previously.[9,10] Single-wave-

Received: May 3, 2014
Published: July 9, 2014

   dx.doi.org/10.1021/ja504125v | *J. Am. Chem. Soc.* 2014, 136, 10989−10995

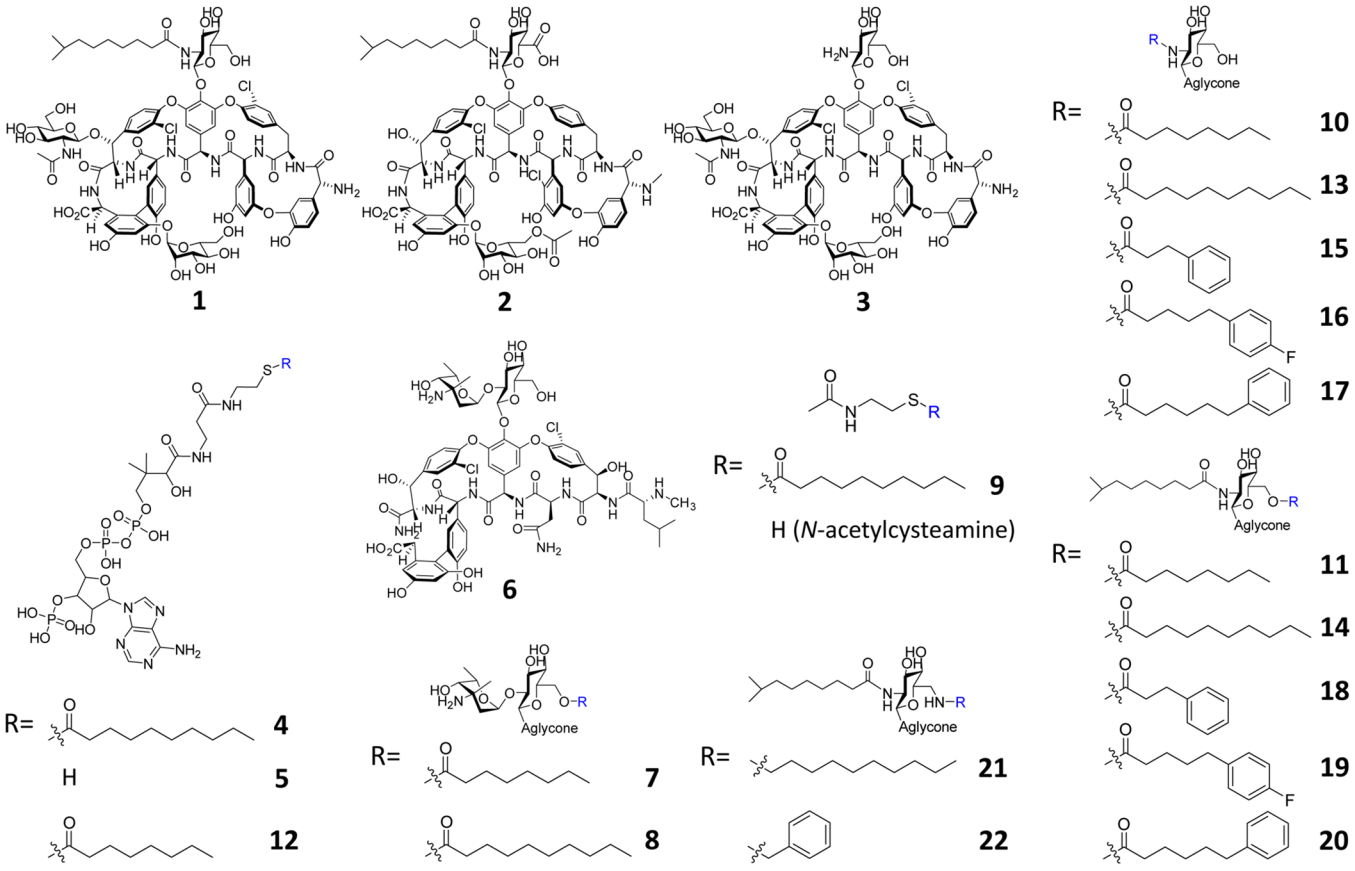

Figure 1. Chemical structures of glycopeptides, acyl-*N*-acetyl cysteamine, and coenzyme A derivatives: teicoplanin A2-2 (Tei, **1**), A40926 (**2**), Tei pseudoaglycone (**3**), decanoyl-CoA (**4**), coenzyme A (CoA, **5**), vancomycin (Van, **6**), octanoyl-derivatized Van (C_8-Van, **7**), decanoyl-derivatized Van (C_{10}-Van, **8**), decanoyl-*N*-acetyl cysteamine (decanoyl-NAC, **9**), octanoyl-substituted Tei (C_8-Tei, **10**), C_8,C_{10}-Tei (**11**), octanoyl-CoA (**12**), decanoyl-Tei (C_{10}-Tei, **13**), C_{10},C_{10}-Tei (**14**), dihydrocinnamoyl-Tei (**15**), 5-(4-fluorophenyl)valeryl-Tei (**16**), 6-phenylhexanoyl-Tei (**17**), 2-*N*-C_{10},6-*O*-dihydrocinnamoyl-Tei (**18**), 2-*N*-C_{10},6-*O*-5-(4-fluorophenyl)valeryl-Tei (**19**), 2-*N*-C_{10},6-*O*-6-phenylhexanoyl-Tei (**20**), 6-*C*-decylaminated Tei (**21**), and 6-*C*-benzylamine-Tei (**22**).

length anomalous dispersion (SAD) and molecular replacement (MR) methods were used to solve structures of native and complexed Orf11*/Dbv8. Mutants were made by using QuikChange. Biochemical analyses for wild-type (WT) protein and mutants were performed using liquid chromatography–mass spectrometry (LC-MS). Structure dynamics were determined by gel filtration chromatography (GFC) and analytical ultracentrifugation (AUC). Substrate–enzyme affinity was determined using isothermal titration calorimetry (ITC). Biological assays were performed according standard protocols. Full details are given in the Supporting Information.

RESULTS AND DISCUSSION

Structure Determination and Domain Arrangement. Due to the lack of structural homologues in public databases, the initial phase was solved using SAD on crystals of selenomethionyl Orf11*, which then served as a search model for other native and ligand-bound data sets in the MR routine. The resolutions of these multiphased structures range from 1.9 to 2.3 Å, with reasonable values of R_{work} and R_{free}, as shown in Table S1. The structures of Orf11*/Dbv8 and complexes thereof all contain one molecule in the asymmetric unit. Analyses by GFC and AUC (Figure S1) suggest that monomers are the most relevant biologically active state for Orf11*/Dbv8, in contrast to GCN5-related *N*-acetyltransferases (GNATs), which are active as dimers.[11−14]

Both Orf11* and Dbv8 fold in a dumbbell-like architecture, with two sizable subdomains—an unusual all-helix N-domain and a GNAT-like C-domain (Figure 2a,b and Figure S2)—joined by a short spacer. The all-helix domain is composed of eight helices (α1−α8) with two helix-turn-helix motifs in tandem (α1−α4), flanking a perpendicular four-helix bromodomain-like central core (α5−α8) (residues 1−170; the numbering system referred to here is that of Orf11* unless otherwise stated), reminiscent of eukaryotic histone acetyltransferase (HAT) complexes.[15−17] Helices α5 and α6 are juxtaposed in parallel, connected transversely by a long loop (residues 84−100), in contrast to the antiparallel arrangement of helices α7 and α8. The GNAT-like domain has a central 5-β-strand core (β1−β5) flanked by two α helices—one short helix (α9) and one fragmented long helix (the latter is composed of four and six short helices for Orf11* and Dbv8, respectively)—on each side. A Dali server search suggests that the N-terminal subdomain of Orf11*/Dbv8 is structurally akin to the AAA+ protein family (ATPases associated with diverse cellular activities) (Figure S3),[18] whereas functionally Orf11*/Dbv8 resembles a miniature of CBP/p300 in the HAT protein family.[19] CBP/p300 houses a large GNAT domain alongside several smaller domains, including a helix-turn-helix and a bromodomain for recruiting acetylated lysine residues in histones. The bromo-like domain in Orf11*/Dbv8 may likewise act to recognize the peptide substrate Tei/A40926 pseudoaglycone (see below). With these unique traits, Orf11*/Dbv8 indeed represents a new architecture in the prokaryotic NAT family.

dx.doi.org/10.1021/ja504125v | J. Am. Chem. Soc. 2014, 136, 10989−10995

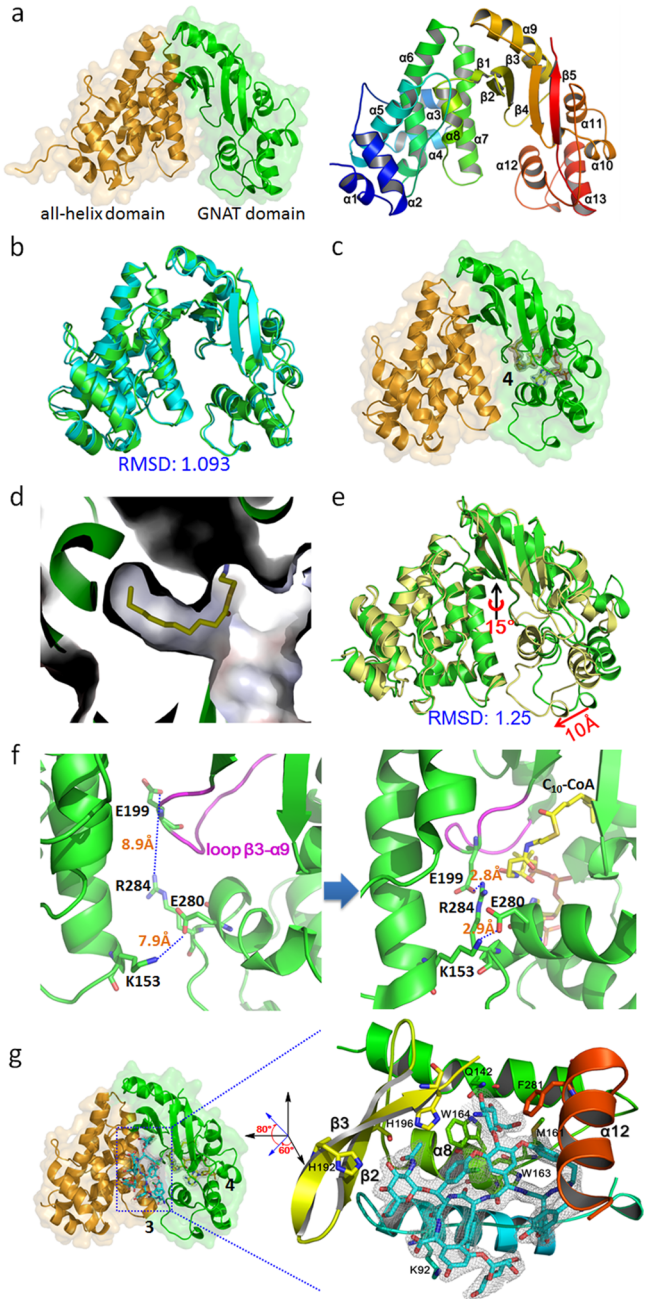

Figure 2. Structures of Orf11* and Dbv8. (a) The apo structure of Orf11*, in which the all-helix domain is colored gold and the GNAT domain is colored green (left panel). The all-helix domain consists of eight α-helices ($\alpha1-\alpha8$); the GNAT domain is composed of a five-stranded β-sheet ($\beta1-\beta5$) and five α-helices ($\alpha9-\alpha13$). (b) Orf11* (green) and Dbv8 (cyan) were superimposed with rmsd = 1.093 Å for 310 Cα. (c) Orf11* in complex with decanoyl-CoA (**4**), which is bound at the GNAT domain. (d) View of the lipid tunnel in Orf11*/Dbv8. (e) Both the unary (green) and binary (gold) structures of Orf11* were superimposed with rmsd = 1.25 Å for 319 Cα. (f) The loop $\beta3-\alpha9$ (purple) in the GNAT domain undergoes a 180° inside-out twist when acyl-CoA enters into its binding site. This wavering connects two salt bridges, E199:R284 (2.8 Å) and K153:E280 (2.9 Å). (g) The ternary structure of Orf11* in complex with Tei pseudoaglycone (**3**) and decanoyl-CoA (**4**). The $2F_o - F_c$ electron density maps are contoured at 1.0σ.

Acyl-CoA Binding and Selectivity. The GNAT domain in Orf11*/Dbv8 differs from the canonical GNAT fold as it lacks the first β strand, and the C-terminus extends with four additional helices ($\alpha10-\alpha13$). β-Strands $\beta3$ and $\beta4$ splay apart at the C-termini, where Pro198 replaces a typical β-bulge.[14−16] In a decanoyl-CoA-complexed binary structure (Figure 2c), the decanoyl-CoA bends in an S-shape, edging in the splayed fingers $\beta3$ and $\beta4$ (Figure S4). The pantetheine moiety contacts the loop $\beta3-\alpha9$; the phosphate groups of 3′,5′-phosphoadenosine are adjacent to the main-chain atoms of the C-terminal helices ($\alpha10-\alpha13$), where the loop $\alpha10-\alpha11$ may function as a makeshift P-loop.[20] The ribose is in a 2′-endo conformation, as commonly observed in acetyltransferase cocrystal structures.[14] The decanoyl moiety extends into a deep and wide tunnel formed by $\beta4$, $\alpha11$, and the loop $\beta4-\alpha10$ (Figure 2d). Except for some steric limitations (the α carbon cannot be branched, and the β carbon cannot be charged), the acyl moiety can be as lengthy or bulky as stearoyl, naphthaleneacetyl, or biphenylacetyl (Table S2), thus making Orf11*/Dbv8 an adaptable enzyme that can generate numerous new glycopeptide analogues. ITC analysis showed that Orf11*/Dbv8 does not bind benzoyl-, malonyl-, and methylmalonyl-CoA, in line with the aforementioned limitations. The dissociation constants (K_d) decline with increasing acyl chain length up to C_{10}, whereas the trend reverses when the chain length exceeds C_{10}, suggesting C_{10} is the optimal length for the enzyme. Interestingly, the K_d's decline again when the chain length extends to C_{16}, suggesting that a longer lipid chain may adopt a new shape to increase the binding affinity (Figure S5).

Conformational Change for Acceptor Binding. Structural superimposition of the free enzyme and the Orf11*−decanoyl-CoA binary complex (rmsd = 1.25 for 319 Cα of Orf11*) reveals that the GNAT domain undergoes a substantial conformational change upon binding of acyl-CoA as opposed to the N-terminal domain, which is unchanged (Figure 2e). The loop $\beta3-\alpha9$ in the GNAT domain twists 180° when acyl-CoA comes close to the binding site. This movement connects two salt bridges (Figure 2f), pulling the GNAT domain toward the all-helix domain. The overall 10 Å displacement (or 15° provided the residue V197 the pivot point) may lead to a closed active conformation in the domain junction, forming the Tei pseudoaglycone binding site (Figure 2e). To accurately locate the Tei pseudoaglycone-binding site, ternary structures in complex with both decanoyl-CoA and Tei pseudoaglycone were attempted. The ternary crystals were successfully obtained only through soaking the decanoyl-CoA-complexed H196A mutant crystals with Tei pseudoaglycone (**3**), suggesting the closed conformation is necessary for pseudoaglycone binding (Figure 2g). An extra cloud of electron density adjacent to acyl-CoA (surrounded by $\beta2$, $\beta3$, $\alpha12$, and the loop $\alpha5-\alpha6$) was identified, which fitted well with Tei pseudoaglycone (**3**). The aglycone scaffold adopts a more compact conformation than those of the Dbv29, ubiquitin, and StaL complexes, in contrast to the relatively flattened conformation of the Orf2* and Teg12 complexes.[7,8,21−23] Superposition of the teicoplanin class glycopeptides further showed that the spatial positioning of the lipid moiety is restricted to the lipid tunnel in the given enzyme, so that the orientation of the liposugar moiety is enzyme-dependent (except the one with ubiquitin, which is not a natural binding host for the teicoplanin class glycopeptides) (Figure S6).

In general, the upper part of the heptapeptide core interacts with the enzyme ($\beta2$, $\beta3$, $\alpha8$, and $\alpha12$) through van der Waals forces, whereas the lower part is free of contact. The central 4Hpg glucosamine is enclosed by a slew of residues (Q142, M161, W163, W164, H196, and F281) but lacks specific interactions,

dx.doi.org/10.1021/ja504125v | J. Am. Chem. Soc. 2014, 136, 10989−10995

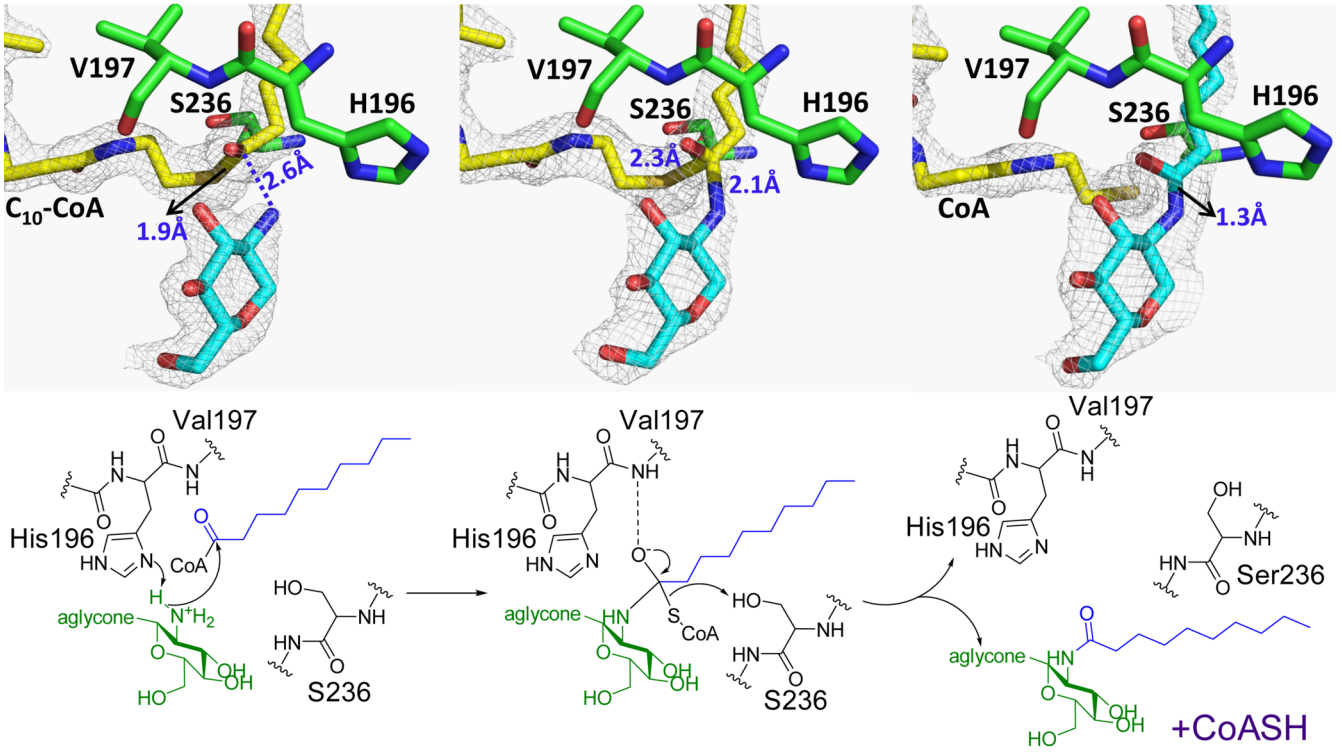

Figure 3. Reaction intermediates and enzymatic mechanisms. (Top) Structural views for three reaction states—pre-acylation (left), tetrahedron intermediate (center), and post-acylation (right)—in three ternary structures. (Bottom) Proposed catalytic mechanism for the Orf11*-mediated acyltransfer reaction. The H196A is modeled back to His196 based on the corresponding geometry at the active site of the binary wild-type structure. The $2F_o - F_c$ electron density maps are contoured at 1.2σ.

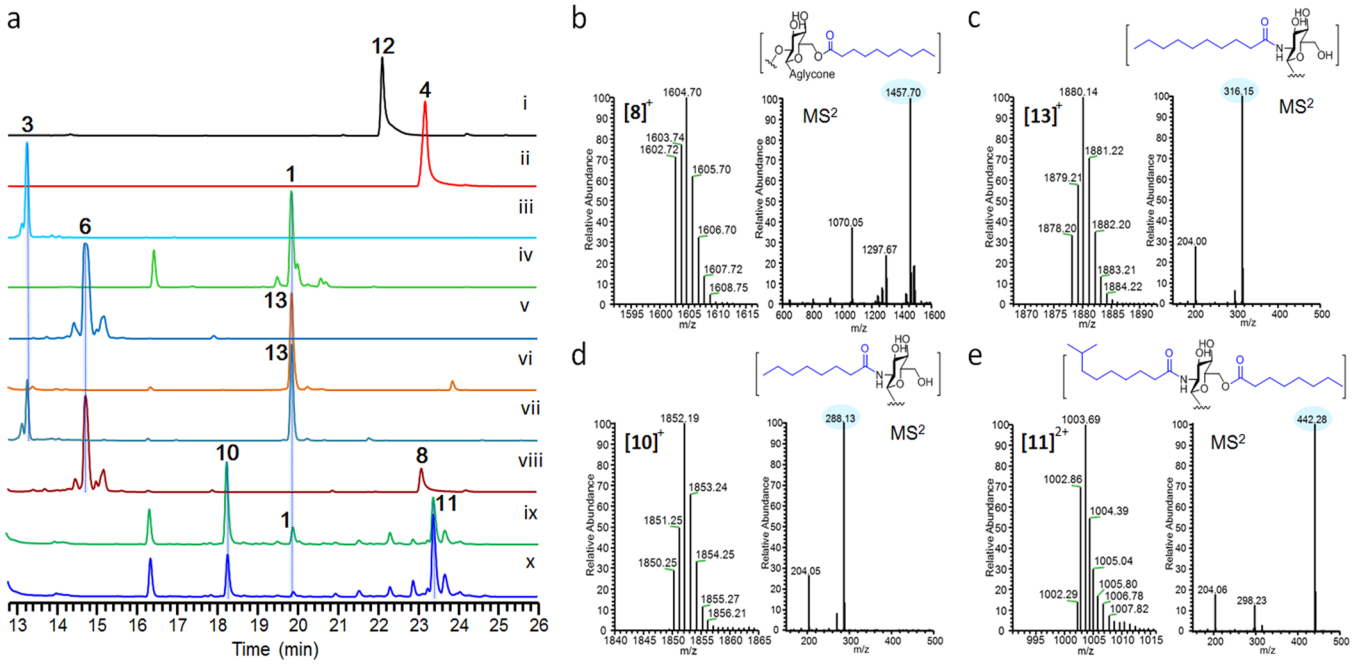

Figure 4. LC traces and mass spectra. (a) LC traces: (i) octanoyl-CoA **12**, (ii) decanoyl-CoA **4**, (iii) Tei pseudoaglycone **3**, (iv) Tei **1** (major: A2-2 and A2-3; minor: A2-1, A2-4, A2-5, and RS1−RS4), (v) Van**6**, (vi) formation of C_{10}-Tei **13** in an enzymatic reaction containing decanoyl-CoA **4** and Tei pseudoaglycone **3**, (vii) formation of C_{10}-Tei **13** in an enzymatic reaction containing decanoyl-NAC **9** and Tei pseudoaglycone **3**, (viii) formation of C_{10}-Van **8** in an enzymatic reaction containing decanoyl-CoA **4** and Van **6**, (ix) formation of C_8-Tei **10** and diacyl-teicoplanin (C_8,C_{10}-Tei) **11** in a reaction at pH 7.0, with 1 equiv of acyl-NAC/Tei in the presence of octanoyl-CoA **12** and Tei **1**; (x) formation of C_8-Tei **10** and diacyl-teicoplanin (C_8,C_{10}-Tei) **11** in a reaction at pH 9.0, with 3 equiv of acyl-NAC/Tei and 30% DMSO in the presence of octanoyl-CoA **12** and Tei **1**. (b−e) Mass and MS^2 spectra for (b) C_{10}-Van **8**, (c) C_{10}-Tei **13**, (d) C_8-Tei **10**, and (e) C_8,C_{10}-Tei **11** (m/z is shown as a doubly charged ion).

dx.doi.org/10.1021/ja504125v | J. Am. Chem. Soc. 2014, 136, 10989−10995

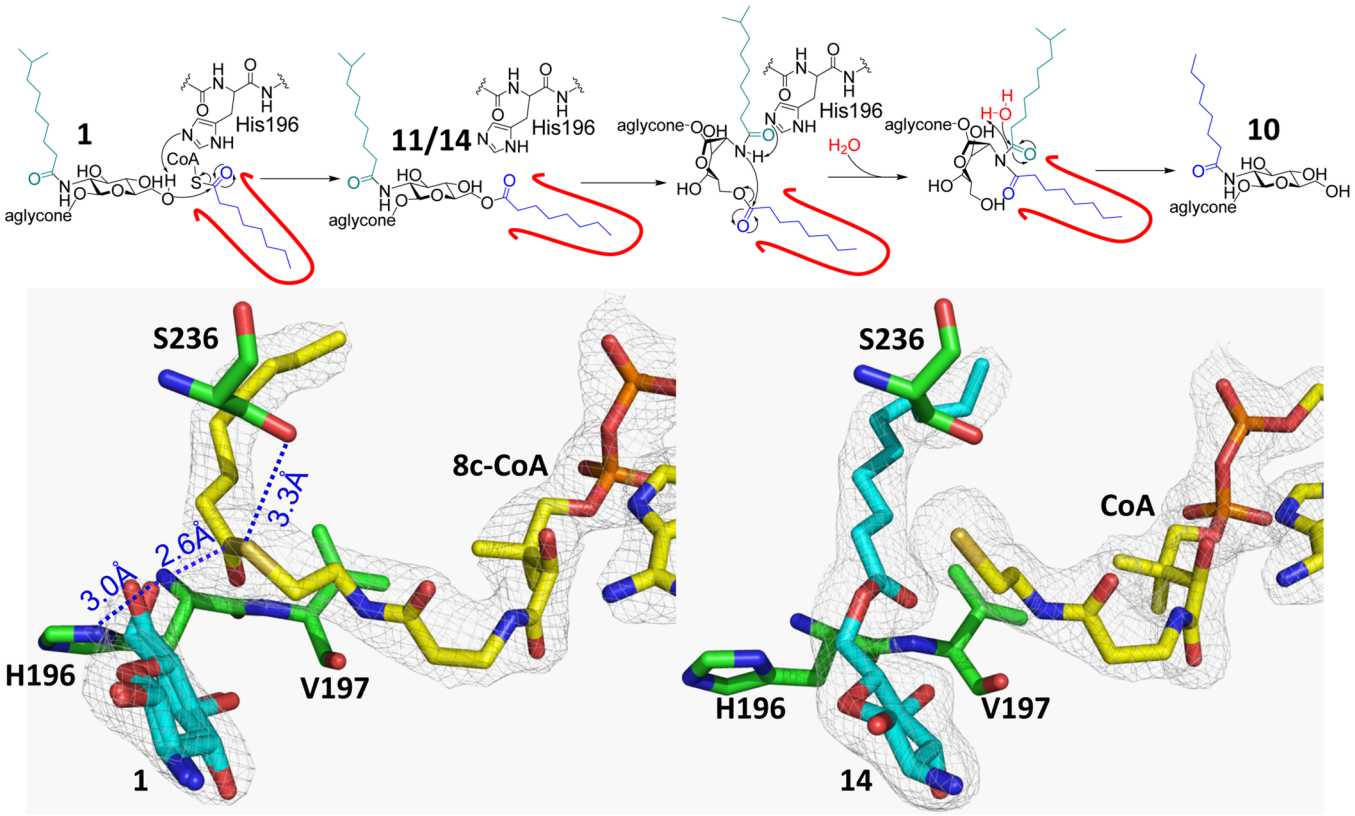

Figure 5. (Top) Proposed mechanism of Orf11*-mediated 1,4-acyl migration reaction. The lipid tunnel in Orf11* is drawn in red. (Bottom) Structural views for the first two acyl migration reaction states: (left) the C6 OH group of glucosamine pointing to the acyl-CoA carbonyl carbon and (right) formation of the C6 *O*-acyl glucosamine bond. The $2F_o - F_c$ electron density maps are contoured at 1.0σ.

suggesting the sugar is less constrained (see below) (Figure S7). ITC analysis supported this observation, as Tei pseudoaglycone (**3**) or CoA (**5**) barely binds to the enzyme, thus suggesting the enzyme assumes an open state (Figure 2e and Figure S5). Superposition of unary, binary, and ternary structures reveals that acyl-CoA rather than CoA plays a pivotal role in configuring the GNAT domain for Tei pseudoaglycone binding (Figure S8).

Acyl Transfer and Migration. It has been well documented that acyl transfer can proceed in two ways, direct transfer and acyl-enzyme-mediated transfer as seen in histone ATs.[14,17] Three reaction states—pre-acylation, tetrahedron intermediate, and post-acylation—were spotted in three individual ternary structures, suggesting that the acyl-transfer reaction of Orf11*/Dbv8 follows the direct transfer mechanism (Figure 3 and Figures S9−S11). Of these complexes, the remarkable tetrahedron intermediate may occur because the H196A mutant is an activity-crippled enzyme. In brief, we propose that H196 acts as the general base, deprotonating the C2 NH^{3+} of the glucosamine at 4Hpg, which then attacks the thioester carbonyl carbon of acyl-CoA. The resulting tetrahedral transition is stabilized by the main-chain amide of V197, where an oxyanion hole likely resides. Collapse of the transition state results in *N*-acylated Tei pseudoaglycone. The departure of CoASH may be facilitated by S236 through protonating the sulfur anion to sulfhydryl. This mechanistic notion was supported by mutagenic and biochemical assays, as relative activities of mutants H196A and H196A/S236A (double-mutation) plunged significantly (5% and 0%, respectively, relative to WT) (Table S3). Acyl-CoA apparently binds to the enzyme first and triggers a protein conformational change to form the Tei pseudoaglycone binding site. Upon completion of the acyl-transfer reaction, CoA likely leaves before the acylated product to enable the enzyme to re-adopt the open state for the next reaction cycle.

Interestingly, the enzyme is capable of *O*-acylating Van at the C6 OH of glucose instead of the C3′ NH_2 of vancosamine on the basis of NMR and MS analysis (**7**/**8**, Figure 4a,b, trace viii, and Figures S12 and S13). The acylation modification has in many cases been shown to be vital to the bioactivities of natural products,[1,3,4] but it would not be cost-effective if the "acyl" liaison needs to be a pricey acyl-CoA. An acyl-CoA mimic, decanoyl-*N*-acetyl cysteamine (decanoyl-NAC **9**, Figure S14), was thus synthesized to see if the minimum element is able to elicit the protein conformational change and thereby serve as an acyl donor. An enzymatic reaction containing Tei pseudoaglycone (**3**) and decanoyl-NAC (**9**) was examined, whereby emergence of a new peak on the LC trace with the same retention time and mass unit as Tei (**1**, A2-3) verified that acyl-NAC is an acyl-CoA surrogate (Figure 4a,c, trace vii). The yield can be further improved if free CoA is included. We reason that the acyl group is exchanged via transesterification from acyl-NAC to free CoA in the active site; in this case CoA switches its role from a substrate/product ligand to an enzyme cofactor. Most strikingly, a double-acylation reaction and an acyl-substitution reaction were discovered, whereby Tei (**1**) can be converted to octanoyl-substituted Tei (C_8-Tei) (**10**) and diacyl-Tei (**11**) (C_8,C_{10}-Tei) in an enzyme reaction in the presence of both Tei (**1**) and octanoyl-CoA (**12**) (Figure 4a,d,e, trace ix). MS and NMR analysis confirmed that compound **11** is 2-*N*-decanoyl-6-*O*-octanoyl-Tei, indicating that compound **10** is formed via compound **11** in the acyl-substituted reaction (Figure 4a,d,e, trace ix, and Figures S15 and S16).

dx.doi.org/10.1021/ja504125v | *J. Am. Chem. Soc.* 2014, 136, 10989−10995

Table 1. MICs of Vancomycin, Teicoplanin, and Analogues versus Testing Strains[a]

	sensitive strains		resistant strains						
			VanA VRE		VanB VRE			VanC VRE	
compd	ATCC 29302 *E. faecalis*	ATCC 33186 *E. faecalis*	ATCC 700221 *E. faecium*	ATCC BAA2320 *E. faecium*	ATCC 51299 *E. faecalis*	ATCC 51575 *E. faecalis*	ATCC 700802 *E. faecalis*	ATCC 700425 *E. gallinarum*	ATCC 700668 *E. casseliflavus*
1	0.125	0.25	>64	>64	0.5	1	0.5	1	1
6	2	2	>64	>64	32	64	64	16	8
10	1	2	>64	>64	2	4	4	8	4
15	8	8	>64	>64	16	32	32	16	16
16	2	2	64	64	4	16	8	8	8
17	1	2	64	64	4	8	4	4	4
11	0.125	0.25	1	4	0.25	0.5	0.5	0.5	0.5
18	0.25	0.5	4	8	0.5	1	0.5	2	1
19	0.125	0.25	2	8	0.25	0.5	0.5	0.125	0.25
20	0.125	0.25	1	4	0.25	0.5	0.5	0.25	0.5
21	0.5	0.5	4	4	0.5	2	2	1	0.5
22	0.25	0.25	2	8	0.5	0.5	0.5	4	2

[a]The concentration unit is μg mL^{-1}. Experiments were performed in duplicate.

We reason that the 2-*N*,6-*O*-diacyl glucosamine moiety, when subjected to intramolecular restraints under the active-site constraints, experiences an equatorial−axial interconversion via the twist-boat state (Figure 5, top panel). In a 1,4-diaxial fashion (a boat conformation), the C6 acyl and the C2 secondary amine are within a bond-length distance, allowing C6→C2 acyl migration to form a geminal diacyl intermediate. Given that the migrated acyl moiety likely remains inside the lipid tunnel, the solvent-exposed C2 *N*-acyl group is more accessible to water attack, resulting in formation of the acyl-substituted Tei (Figure 5, top panel). To verify this working model, two additional crystal structures were solved by soaking Tei (**1**) into the acyl-CoA/Orf11* binary crystals. The electron densities for both the C2 *N*-acyl and aglycone moieties are too faint to be modeled, likely due to larger molecular oscillation (Tei gaining less binding entropy than pseudoaglycone in ITC analysis), whereas the electron density of the glucosamine moiety is well defined, with the C6 OH clearly pointing to the acyl-CoA carbonyl carbon in one structure and with formation of a C6 *O*-acyl bond in the other (Figure 5, bottom panel, and Figures S17 and S18), backing up the first two stages in the working model. We further examined acyl-Van (**7**), of which no new product was found, suggesting that the substitution reaction very likely follows the intramolecular hexose-chair-flipping mechanism. We went on to examine the reaction conditions in a bid to control the reaction. One set of conditions (pH 7.0, 1 molar equiv of acyl-NAC/Tei) gives a ratio of 4:1 for acyl-substituted Tei versus diacyl Tei; the ratio is reversed (1:4) in another condition set of conditions (pH 9.0, 3 molar equiv of acyl-NAC/Tei, 30% DMSO). Overall, the conversion is a mild and effective one-step reaction, whereby the final yield is high because the minor product is recyclable in each condition. We reason that the reaction mechanism is a synergy of stoichiometric and solvational effects (Figure 4a, traces ix and x).

Biological Activities of New Analogues. This study affords an expedient way to generate new Tei analogues without problematic deacylation and reacylation processes.[7,8,24] This finding also provides a one-pot solution to convert Tei mixtures (A2-1−A2-5, RS1−RS4, etc.)[2] of natural isolates to a single uniform compound, which should facilitate the development of approvable drugs (teicoplanin in mixtures is one of the reasons it is not approved by the U.S. FDA; see Figure 4a, traces iv, vi, and vii).[10] Having been able to add new chemical functionality with our modified teicoplanin analogues, we wanted to examine whether we had similarly expanded new biological functionality; accordingly, we determined the minimum inhibition concentrations (MICs) of several of the compounds against collections of major types (VanABC) of vancomycin-resistant enterococcus (VRE) (Table 1). We observed that, in general, the VanA type is more drug-resistant than the VanBC types. The inhibition is slightly decreased with an additional phenyl ring at the terminus of C2 *N*-acyl at various lengths (*N*-acyl-substituted Tei **10**, **15**, **16**, and **17**) as compared to teicoplanin (**1**). The 2*N*,6*O*-diacyl analogues (**11**, **18**, **19**, and **20**), however, showed significantly enhanced bactericidal activities against all nine tested strains (both sensitive and resistant strains) when compared to mono-*N*-acyl-substituted Tei, vancomycin, and teicoplanin. By looking into the bactericidal variations among these diacyl analogues, we see that the straight-chain octanoyl analogue **11** slightly outperformed the phenylpropionyl analogue (**18**), which however is compensated by increasing the chain length (analogues **19** and **20**). VanC VRE is more sensitive to analogue **19**, wherein the fluorine substituent at the *para* position of the phenyl ring may exert some electronic influences; both the straight-chain analogue **11** and the phenylhexanoyl analogue **20** are more effective against VanA VRE. Compared with the decylamine analogue **21** and the benzylamine analogue **22**, which were reported to have superb bactericidal activities,[8] the present ester analogues as a whole out-do even these amine analogues, possibly because of subtle stereoelectronic differences between the amine and the ester functional groups with cell-wall precursors/components at physiological conditions. Our findings indeed complement/expand the work reported by Thorson and co-workers, where the glucose C3′ or C4′ is the optimal position for neoglycopeptide lipidation.[25] In connection with glycorandomization, diversification of the glycolipid portion of lipoglycopeptide antibiotics would supersede the effectiveness of vancomycin/teicoplanin against VRE/MRSA.[26]

In summary, the development of new antibiotics with enhanced or broadened antimicrobial efficacy remains a pressing and challenging goal. Elucidation of the key long-aliphatic *N*-acyltransferase complexes in the biosynthesis of the clinically important antibiotic teicoplanin/A40926 not only resolved the difficult problems but also gave details beyond the enzyme's ordinary task. We anticipate that the broad-substrate acyl-

dx.doi.org/10.1021/ja504125v | J. Am. Chem. Soc. 2014, 136, 10989−10995

transfer, diacyl-transfer, and acyl-substitution reactions identified herein will offer a valuable way to make more effective and synthetically challenging biochemicals to meet high synthetic and medicinal demands.

■ ASSOCIATED CONTENT

Supporting Information

Detailed experimental procedures, data processing and structure refinement statistics, and supplementary figures and tables. This material is available free of charge via the Internet at http://pubs.acs.org. The coordinates have been deposited in the Protein Data Bank under the following accession codes: Se-Orf11*, 4MFJ; Orf11*H196A/decanoyl-CoA, 4MFK; Orf11*H196A/decanoyl-CoA/Tei pseudoaglycone, 4MFL; Orf11*H196A/decanoyl-CoA-Tei pseudoaglycone, 4MFP; Orf11*H196A/CoA/10C-teicoplanin, 4MFQ; Dbv8/decanoyl-CoA, 4MFZ; Orf11*/octanoyl-CoA/teicoplanin, 4Q36; and Orf11*/CoA/O6-decanoyl glucosamine, 4Q38.

■ AUTHOR INFORMATION

Corresponding Author

tlli@gate.sinica.edu.tw

Notes

The authors declare no competing financial interest.

■ ACKNOWLEDGMENTS

We are grateful to Ministry of Science and Technology, Taiwan (100-2311-B-001-018-MY3), the National Health Research Institute (NHRI-EX101-10118NC), and Academia Sinica (intramural funding) for funding this work. Portions of this research were carried out at the National Synchrotron Radiation Research Center (NSRRC), a national user facility supported by the National Science Council of Taiwan, ROC. The Synchrotron Radiation Protein Crystallography Facility is supported by the National Research Program for Genomic Medicine. We thank both NSRRC of Taiwan and SPring-8 of Japan for beam time allocations

■ REFERENCES

(1) Nicolaou, K. C.; Boddy, C. N.; Brase, S.; Winssinger, N. *Angew. Chem., Int. Ed.* **1999**, *38*, 2096.
(2) Li, T. L.; Huang, F.; Haydock, S. F.; Mironenko, T.; Leadlay, P. F.; Spencer, J. B. *Chem. Biol.* **2004**, *11*, 107.
(3) Kahne, D.; Leimkuhler, C.; Lu, W.; Walsh, C. *Chem. Rev.* **2005**, *105*, 425.
(4) Kruger, R. G.; Lu, W.; Oberthur, M.; Tao, J.; Kahne, D.; Walsh, C. T. *Chem. Biol.* **2005**, *12*, 131.
(5) Howard-Jones, A. R.; Kruger, R. G.; Lu, W.; Tao, J.; Leimkuhler, C.; Kahne, D.; Walsh, C. T. *J. Am. Chem. Soc.* **2007**, *129*, 10082.
(6) Li, Y. S.; Ho, J. Y.; Huang, C. C.; Lyu, S. Y.; Lee, C. Y.; Huang, Y. T.; Wu, C. J.; Chan, H. C.; Huang, C. J.; Hsu, N. S.; Tsai, M. D.; Li, T. L. *J. Am. Chem. Soc.* **2007**, *129*, 13384.
(7) Chan, H. C.; Huang, Y. T.; Lyu, S. Y.; Huang, C. J.; Li, Y. S.; Liu, Y. C.; Chou, C. C.; Tsai, M. D.; Li, T. L. *Mol. Biosyst.* **2011**, *7*, 1224.
(8) Liu, Y. C.; Li, Y. S.; Lyu, S. Y.; Hsu, L. J.; Chen, Y. H.; Huang, Y. T.; Chan, H. C.; Huang, C. J.; Chen, G. H.; Chou, C. C.; Tsai, M. D.; Li, T. L. *Nat. Chem. Biol.* **2011**, *7*, 304.
(9) Huang, Y. T.; Lyu, S. Y.; Chuang, P. H.; Hsu, N. S.; Li, Y. S.; Chan, H. C.; Huang, C. J.; Liu, Y. C.; Wu, C. J.; Yang, W. B.; Li, T. L. *ChemBioChem* **2009**, *10*, 2480.
(10) Li, T. L.; Spiteller, D.; Spencer, J. B. *ChemBioChem* **2009**, *10*, 896.
(11) Lin, Y.; Fletcher, C. M.; Zhou, J.; Allis, C. D.; Wagner, G. *Nature* **1999**, *400*, 86.
(12) Rojas, J. R.; Trievel, R. C.; Zhou, J.; Mo, Y.; Li, X.; Berger, S. L.; Allis, C. D.; Marmorstein, R. *Nature* **1999**, *401*, 93.
(13) Syntichaki, P.; Topalidou, I.; Thireos, G. *Nature* **2000**, *404*, 414.
(14) Vetting, M. W.; LP, S. d. C.; Yu, M.; Hegde, S. S.; Magnet, S.; Roderick, S. L.; Blanchard, J. S. *Arch. Biochem. Biophys.* **2005**, *433*, 212.
(15) Dyda, F.; Klein, D. C.; Hickman, A. B. *Annu. Rev. Biophys. Biomol. Struct.* **2000**, *29*, 81.
(16) Marmorstein, R. *J. Mol. Biol.* **2001**, *311*, 433.
(17) Marmorstein, R.; Roth, S. Y. *Curr. Opin. Genet. Dev.* **2001**, *11*, 155.
(18) Hanson, P. I.; Whiteheart, S. W. *Nat. Rev. Mol. Cell. Biol.* **2005**, *6*, 519.
(19) Das, C.; Lucia, M. S.; Hansen, K. C.; Tyler, J. K. *Nature* **2009**, *459*, 113.
(20) Verstraeten, N.; Fauvart, M.; Versees, W.; Michiels, J. *Microbiol. Mol. Biol. Rev.* **2011**, *75*, 507.
(21) Economou, N. J.; Nahoum, V.; Weeks, S. D.; Grasty, K. C.; Zentner, I. J.; Townsend, T. M.; Bhuiya, M. W.; Cocklin, S.; Loll, P. J. *J. Am. Chem. Soc.* **2012**, *134*, 4637.
(22) Shi, R.; Munger, C.; Kalan, L.; Sulea, T.; Wright, G. D.; Cygler, M. *Proc. Natl. Acad. Sci. U.S.A.* **2012**, *109*, 11824.
(23) Bick, M. J.; Banik, J. J.; Darst, S. A.; Brady, S. F. *Biochemistry* **2010**, *49*, 4159.
(24) Li, T. L.; Liu, Y. C.; Lyu, S. Y. *Curr. Opin. Chem. Biol.* **2012**, *16*, 170.
(25) Griffith, B. R.; Krepel, C.; Fu, X.; Blanchard, S.; Ahmed, A.; Edmiston, C. E.; Thorson, J. S. *J. Am. Chem. Soc.* **2007**, *129*, 8150.
(26) Fu, X.; Albermann, C.; Jiang, J.; Liao, J.; Zhang, C.; Thorson, J. S. *Nat. Biotechnol.* **2003**, *21*, 1467.